Journal of Colloid and Interface Science 450 (2015) 168–173

Contents lists available at ScienceDirect

Journal of Colloid and Interface Science

www.elsevier.com/locate/jcis

PdCo alloy nanoparticle–embedded carbon nanofiber for ultrasensitive nonenzymatic detection of hydrogen peroxide and nitrite

Dong Liu [a], Qiaohui Guo [a], Xueping Zhang [a], Haoqing Hou [b], Tianyan You [a,*]

[a] State Key Laboratory of Electroanalytical Chemistry, Changchun Institute of Applied Chemistry, Chinese Academy of Sciences, Jilin 130022, China
[b] College of Chemistry and Chemical Engineering, Jiangxi Normal University, Jiangxi 330027, China

GRAPHICAL ABSTRACT

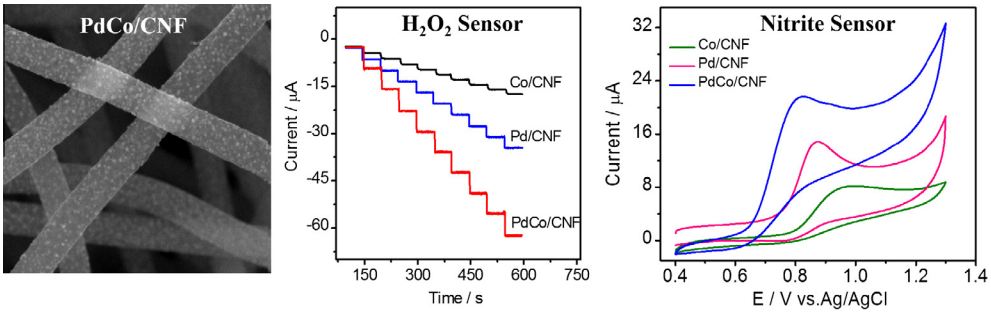

ARTICLE INFO

Article history:
Received 10 February 2015
Accepted 6 March 2015
Available online 16 March 2015

Keywords:
Electrochemistry
PdCo alloy nanoparticle
Carbon nanofiber
Biosensor

ABSTRACT

PdCo alloy nanoparticle–embedded carbon nanofiber (PdCo/CNF) prepared by electrospinning and thermal treatment was employed as a high-performance platform for the determination of hydrogen peroxide and nitrite. The as-obtained PdCo/CNF were characterized by transmission electron microscopy, energy-dispersive X-ray spectroscopy and X-ray diffraction. Electrochemical impedance spectroscopy, cyclic voltammetry and differential pulse voltammetry were employed to investigate the electrochemical behaviors of the resultant biosensor. The proposed PdCo/CNF-based biosensor showed excellent analytical performances toward hydrogen peroxide (detection limit: 0.1 μM; linear range: 0.2 μM–23.5 mM) and nitrite (detection limit: 0.2 μM; linear range: 0.4–30 μM and 30–400 μM). The superior analytical properties could be attributed to the synergic effect and firmly embedment of well-dispersed PdCo alloy nanoparticles. These attractive electrochemical properties make this robust electrode material promising for the development of effective electrochemical sensors.

© 2015 Elsevier Inc. All rights reserved.

1. Introduction

The development of methods for the detection of hydrogen peroxide (H_2O_2) with high reliability has received considerable attentions in various fields [1–4]. As a reactive oxygen species, H_2O_2 is an important by-product for numerous enzymatic reactions, and also take an essential role in the regulation of various biological processes [5,4]. Electrochemical method has been extensively explored for the fabrication of H_2O_2 biosensors as a simple and economic method. Particularly, enzyme-based electrochemical biosensors for H_2O_2 detection have been considered as the most effective approach for their excellent sensitivity and selectivity. However, the poor long-term stability as well as high cost is a serious problem for these enzymatic biosensors [6]. Lots of investigations are focused on nonenzymatic H_2O_2 biosensors due to the comparable sensitivity and selectivity but significantly enhanced stability. Among these studies, Pd-based nanostructures have demonstrated

* Corresponding author. Fax: +86 431 85262850.
E-mail address: youty@ciac.jl.cn (T. You).

http://dx.doi.org/10.1016/j.jcis.2015.03.014
0021-9797/© 2015 Elsevier Inc. All rights reserved.

their advantages for the construction of nonenzymatic H_2O_2 biosensors. For example, You et al. fabricated a nonenzymatic H_2O_2 biosensor by MWCNTs-Pd nanoparticles [7]; Han et al. prepared the spherical porous Pd nanoparticle for the determination of H_2O_2 with a detection limit of 0.68 μM [8]; Jiang et al. employed poly(3,4-ethylenedioxythiophene) nanospheres loaded with 4.5 nm Pd nanoparticles for the H_2O_2 detection which show a low detection limit of 2.84 μM in the range of 2.5×10^{-3}–1.0 mM [9]. In fact, transition metals, such as Pd, are reported to be capable of adopting the oxidation states or adsorbing substances to their surface and further activate the adsorbates [4]. Considering the excellent electrochemical performances of Pd nanoparticles, our group synthesized Pd nanoparticles-load carbon nanofibers (Pd/CNF) by the combination of electrospinning and thermal treatment, and the resultant Pd/CNF presented superior stability with a relatively low detection limit of 0.2 μM toward H_2O_2 [10]. As for the further study, considerable efforts have been aimed at how to improve the sensitivity and selectivity of nonenzymatic H_2O_2 biosensors.

Recently years, growing attention has been paid on bimetallic nanostructures for their controllable surface properties, tailorable atomic and electronic structures, and enhanced electrocatalytic activity, selectivity and stability [11]. With the advent of new synthetic routes and surface analyzing techniques, it has become possible to design and prepare bimetallic systems with desired properties. Pd-based bimetallic nanostructures are explored for highly sensitive biosensing. For instance, Dong's group reported nonenzymatic analysis of glucose at PdM (M = Pt, Au) bimetallic alloy nanowires modified electrode with significantly enhanced sensitivity compared with the monometallic components [12]. Sun et al. constructed a hydrogen peroxide sensor with dumbbell-like Pt_xPd_{100-x}–Fe_3O_4 nanoparticles. Interestingly, they found that the electrocatalytic performance of Pt_xPd_{100-x}–Fe_3O_4 hybrid toward hydrogen peroxide reduction was composition dependent, with $Pt_{48}Pd_{52}$–Fe_3O_4 being the most efficient catalyst [13]. Meng and his co-workers reported Pd–Ag bimetallic dendrites toward 4-nitrophenol reduction with fourfold higher catalytic activity than the corresponding monometallic dendrites [14]. Additionally, further research has confirmed that alloying Pd with transition metal can improve the catalytic activity as well as reduce the cost of the catalyst. Pd–Fe [15], Pd–Co [16,17], and Pd–Ni [18] alloys have been explored as novel electrode materials in oxygen reduction reactions and fuel cell technologies with significantly improved reaction kinetics. Very recently, our group reported PdCo alloy NPs-embedded carbon nanofiber (PdCo/CNF) composites as high-performance electrocatalyst for fuel cells [19]. Compared with Pd/CNF, PdCo/CNF exhibited significantly enhanced electrocatalytic activity and stability due to the synergic effect of bimetallic nanoparticles.

In this work, PdCo/CNF composites are explored for the fabrication of biosensors for the determination of H_2O_2 and nitrite. The unique "embedded" nanostructure may be fairly favorable for the highly sensitive and stable biosensing. Different kinds of important electroactive compounds (e.g., probe molecule (potassium ferricyanide), H_2O_2, and nitrite) are employed to study their electrochemical performances at PdCo/CNF modified carbon paste electrode (PdCo/CNF-CPE). It is found that the modified electrode showed more favorable electron transfer kinetics and much enhanced electrocatalytic activity, which provide a robust and advanced electrode material with great promise for electrochemical sensors and biosensors design.

2. Experimental section

2.1. Reagents and materials

Polyacrylonitrile (PAN), palladium acetylacetonate ($Pd(acac)_2$) and cobalt acetylacetonate ($Co(acac)_2$) were purchased from Sigma–Aldrich. 0.1 M pH 7.0 phosphate buffer solution (PBS) was prepared by mixing Na_2HPO_4 and NaH_2PO_4 solution. Dimethylformamide (DMF), nitrite ($NaNO_2$) and hydrogen peroxide (H_2O_2, 30%) were obtained from Beijing Chemical Co. (China). Doubled-distilled water from millipore system was used throughout the experiment.

2.2. Apparatus

The scanning electron microscopy (SEM) experiments were performed on a PHILIPS XL-30 ESEM (accelerating voltage: 20 kV). The transmission electron microscopy (TEM) images were obtained on a JEOL 2000 TEM at 200 kV (JEOL, Japan). Energy-dispersive X-ray spectroscopy (EDX) analysis with a PHILIPS XL-30 ESEM was employed for chemical composition. X-ray diffraction (XRD) analysis was obtained from a Bruker D8 ADVANCE instrument with Cu Kα radiation (40 kV, 40 mA). UV/vis absorption spectra were recorded on a Perkin-Elmer-950 spectrometer. Electrochemical impedance spectroscopy (EIS) was performed on a Solartron Electrochemical Interface 1286 and Solartron Frequency Response Analyzer (FRA) 1255B. All electrochemical measurements were performed using a CHI 832 electrochemical workstation (Shanghai, China) with a conventional three-electrode system composed of a Ag/AgCl (saturated KCl) as reference, a platinum wire as counter and bare or modified carbon paste electrode (CPE) as working electrode.

2.3. Preparation of PdCo/CNF composites

The PdCo/CNF composite were obtained through the carbonization of $Pd(acac)_2$/$Co(acac)_2$/PAN nanofibers as our previous work [19]. Briefly, the electrospun solution was obtained by dissolving $Pd(acac)_2$, $Co(acac)_2$ and PAN in DMF. $Pd(acac)_2$/$Co(acac)_2$/PAN nanofibers obtained were further carbonized at 850 °C in N_2 for 0.5 h. The Co/CNF and Pd/CNF composites were obtained by the same process.

2.4. Electrode preparation

CPE was prepared by graphite powder and mineral oil employing a copper wire for the electrical contact. 10 μL 1 g mL^{-1} PdCo/CNF suspension was cast on the surface of CPE and dried at room temperature.

3. Results and discussions

3.1. Characterization of PdCo/CNF composites

The as-prepared PdCo/CNF composites were characterized by scanning electron microscopy (SEM) and transmission electron microscopy (TEM). The diameters of CNF ranged from 400 to 500 nm with tens of micrometers in length, and large amounts of NPs were firmly dispersed on or in CNF (Fig. 1A). It was found that uniform PdCo alloy NPs were strongly encapsulated in CNF with narrow size distribution (Fig. 1B and C), and the mean diameter was 26.8 nm. Moreover, the PdCo alloy NP possesses good crystallinity and well-resolved lattice fringes (Fig. 1D). The interplanar spacing of lattice fringes was measured to be 0.214 nm, assigning to the (1 1 1) planes of PdCo alloys. The firm embedment and isolation of PdCo alloy NPs by CNF may contribute to the good dispersibility, leading to high resistance toward sintering [20].

Energy-dispersive X-ray spectroscopy (EDX) and X-ray diffraction (XRD) analysis were conducted to investigate the composition and crystal structure of PdCo/CNF. The corresponding EDX spectrum of PdCo/CNF shows the peaks assigning to C, O, Pd and Co

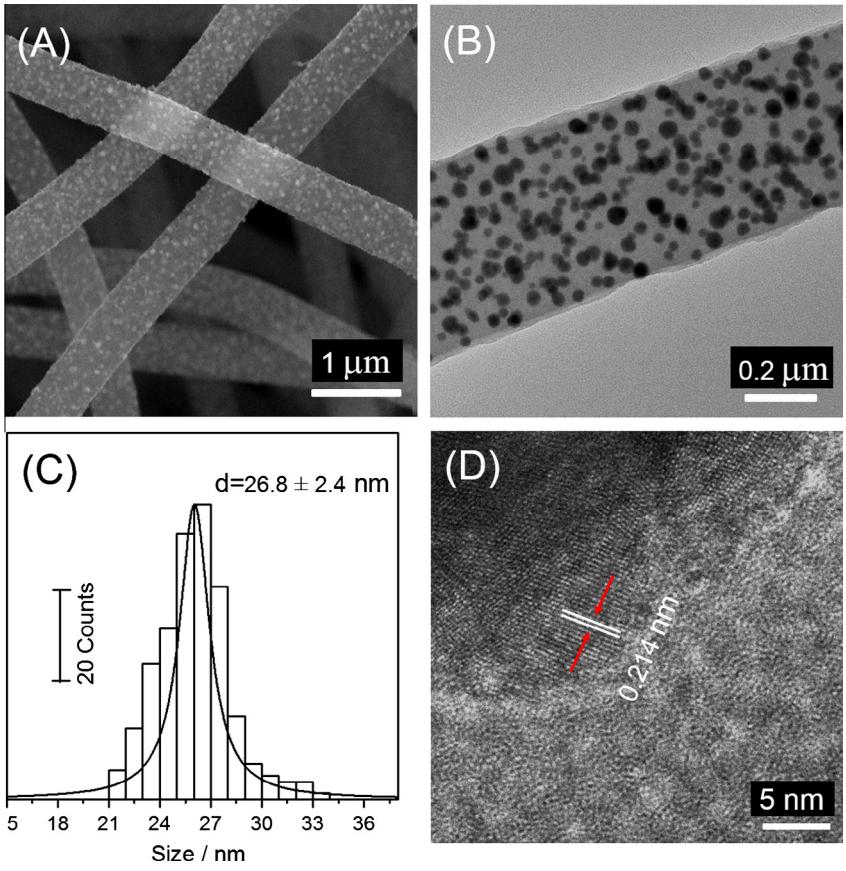

Fig. 1. SEM (A), TEM (B), HRTEM (D) images of PdCo/CNF composite, and (C) is the size distribution of PdCo alloy NPs.

elements, and the atomic ratio of Pd to Co was 49.5:50.5, which is good agreement with the original ratio (Fig. S1). No peak split or impurity was observed according to the XRD results (not shown here), confirming the formation of face-centered cubic (fcc) PdCo alloys. Additionally, the crystalline size of PdCo alloy NPs evaluated from Scherrer formula was 28.2 nm, which is consistent with the TEM result.

3.2. Electrochemical activity and H_2O_2 sensing

Electrochemical impedance spectroscopy (EIS) is an efficient tool for studying the interface properties of modified electrode. Ferricyanide redox probe was selected to evaluate the electrochemical properties of PdCo/CNF-CPE. It is well known that the semicircle diameter of EIS represents the electron transfer resistance (R_{ct}), which controls the electron transfer kinetics of the redox probe at the electrode interface [21]. The R_{ct} of PdCo/CNF-CPE (53.8 Ω) decreased compared with Pd/CNF-CPE (74.2 Ω) and Co/CNF-CPE (96.4 Ω) electrodes (Fig. S2), implying that there is a synergistic effect between Pd and Co in PdCo alloy NPs, which could facilitate the electron transfer.

The voltammetric responses of H_2O_2 at different electrode are shown in Fig. 2. Minor current response corresponding to the reduction of H_2O_2 was observed at bare CPE electrode (Fig. 2A). While at Co/CNF-CPE and Pd/CNF-CPE electrodes, the reduction peak potentials were observed at −0.26 and −0.05 V with larger anodic peak currents upon the addition of 1 mM H_2O_2, respectively (Fig. 2B and C). In the case of PdCo/CNF-CPE electrode (Fig. 2D), lower overpotential (−0.03 V) with much higher reduction current were found compared with that of Co/CNF-CPE and Pd/CNF-CPE electrodes. The enhancement of the electrochemical activities to H_2O_2 may be attributed to the synergistic effect of Pd and Co NPs [22].

Amperometric detection of H_2O_2 was performed to further estimate the analytical properties of PdCo/CNF-CPE. As shown in Fig. 3A, fast response with 95% of steady-state current could be achieved within 2 s at PdCo/CNF-CPE. PdCo/CNF-CPE electrode showed the highest sensitivity (6.64 μA mM^{-1}) as compared with Pd/CNF-CPE (3.89 μA mM^{-1}) and Co/CNF-CPE (1.57 μA mM^{-1}) electrodes (Fig. 3B).

Fig. 4 shows the typical amperometric responses of PdCo/CNF-CPE electrode upon successive addition of H_2O_2 into N_2-saturated PBS (0.1 M, pH 7.0). It can be clearly observed that even after successive additions of different concentrations of H_2O_2 for 50 times, the electrode still keeps steady response, demonstrating that it was a good candidate for consecutive detecting H_2O_2 (Fig. 4A and B). A wide linear range of 0.2 μM–23.5 mM with detection limit (LOD) of 0.1 μM ($S/N = 3$) was obtained (Fig. 4C). For comparison, the analytical parameters obtained with different H_2O_2 sensors were listed in Table 1. The overpotential for the reduction of H_2O_2 at the modified electrode is significantly lower than that at Pd/MCNs modified electrode [23], and AuNPs/graphene/CS modified Au electrode [29]. Moreover, the LOD of H_2O_2 achieved at PdCo/CNF-CPE electrode is much lower than those of state-of-art H_2O_2 sensors reported previously, which was an attractive feature for the determination of H_2O_2 at low concentrations. This wider linear range and higher sensitivity arise from the 3D network structure of the PdCo/CNF film on the electrode surface and the high electrocatalytic activity of PdCo alloy NPs embedded in CNF. Importantly, this direct detection method at PdCo/CNF-CPE can overcome the drawback of the inactivation and leakage for the peroxidase-based or mediator based H_2O_2 sensors.

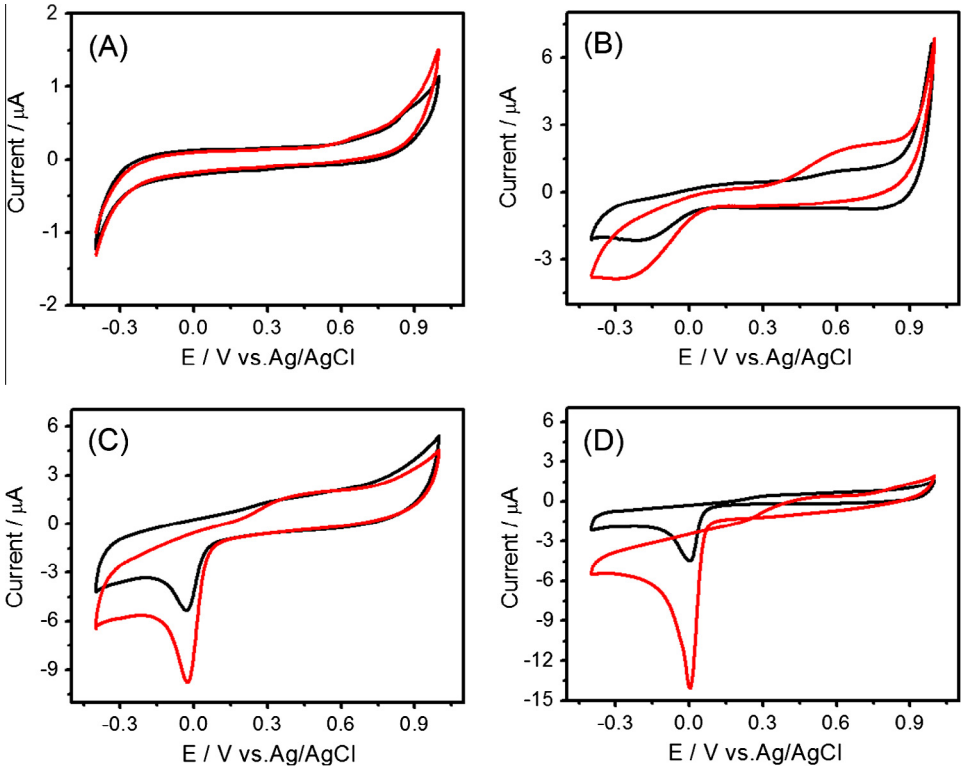

Fig. 2. CVs of bare CPE (A), Co/CNF-CPE (B), Pd/CNF-CPE (C) and PdCo/CNF-CPE (D) electrodes in N_2-saturated 0.1 M PBS (pH 7.0) containing 0 (black line) and 1 mM (red line) H_2O_2, scan rate: 50 mV s^{-1}. (For interpretation of the references to color in this figure legend, the reader is referred to the web version of this article.)

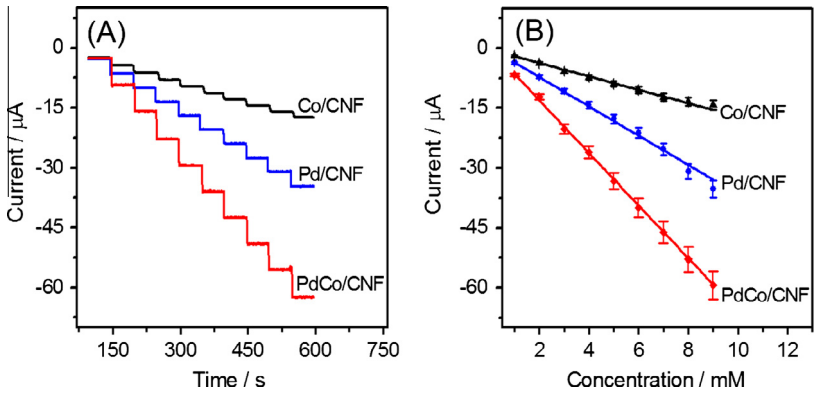

Fig. 3. (A) I–t curves of Co/CNF-CPE, Pd/CNF-CPE and PdCo/CNF-CPE electrodes with successive additions of 1 mM H_2O_2 at −0.15 V, and (B) the corresponding calibration plots (n = 3) for H_2O_2 in N_2-saturated 0.1 M PBS (pH 7.0).

In addition, PdCo/CNF-CPE shows a very high selectivity for the detection of H_2O_2. It was found that 0.15 mM ascorbic acid (AA) and 0.35 mM uric acid (UA) did not show interference to 0.1 mM H_2O_2 (Fig. 4D). The PdCo/CNF-based H_2O_2 sensor also exhibits a good long-term stability. The catalytic current response can maintain over 96% of its initial value after one month. Therefore, by combination of the advantages of good analytical performances and simple preparation procedure, the proposed PdCo/CNF-CPE electrode is promising for the development of effective H_2O_2 sensors.

3.3. Electrochemical activity and nitrite sensing

The PdCo/CNF was also found to exhibit high electrocatalytic activity for the oxidation of nitrite. Fig. 5 depicted CVs obtained at bare CPE and modified CPE electrodes in 0.1 M PBS (pH 4.0) in the presence of 0.5 mM nitrite. At bare CPE electrode (curve a), a weak and broad oxidation peak at 1.14 V was observed, corresponding to the oxidation of NO^{2-} to NO^{3-} through a two-electron oxidation process [30]. After modifying with Co/CNF (curve b) and Pd/CNF (curve c) composite, the oxidation peak currents increased notably, and oxidation peak potentials negatively shift to 0.98 and 0.87 V. The overpotential toward nitrite oxidation further decreased at PdCo/CNF-CPE (0.81 V), and the oxidation peak current (curve d) was 1.6- and 3.0-fold larger than that of Pd/CNF-CPE and Co/CNF-CPE electrodes, respectively. The control experiment of PdCo/CNF-CPE electrode in black 0.1 M PBS (pH 4.0) solution indicated only a background current was found, verifying that the oxidation peak arises from the oxidation of nitrite (Fig. 5, inset). Much higher oxidation peak current and lower

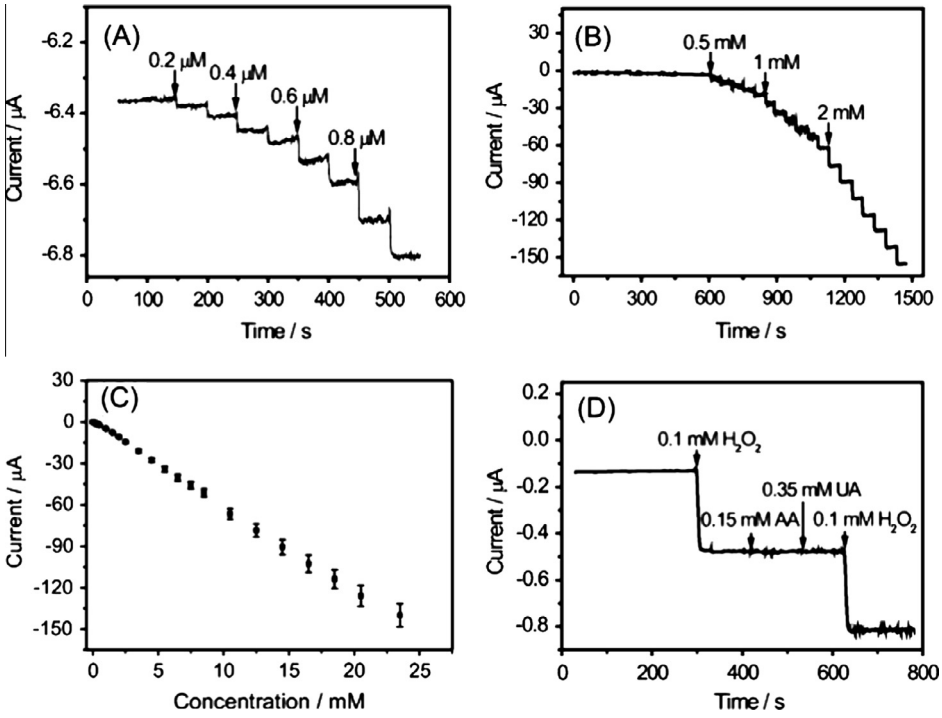

Fig. 4. *I–t* responses of PdCo/CNF-CPE on successive addition low concentration (A), and different concentrations (B) of H_2O_2 into N_2-saturated PBS (0.1 M, pH 7.0). (C) The calibration plot for H_2O_2 detection ($n = 3$). (D) *I–t* responses of PdCo/CNF-CPE to the sequential additions of 0.1 mM H_2O_2, 0.15 mM AA, 0.35 mM UA, and 0.1 mM H_2O_2 into N_2-saturated PBS (0.1 M, pH 7.0). Applied potential: −0.15 V.

Table 1
Analytical parameters of different H_2O_2 sensors.

H_2O_2 sensor	Applied potential (V)	LOD (μM)	Linear range (mM)	Reference
Pd/MCNs[a]	−0.3	1.0	0.0075–10	[23]
MnO_2/VACNTs[b]	0.45	0.8	0.0012–1.8	[24]
PtSe/GCE	0	3.1	0.01–15	[25]
Pt/CNF	0	0.6	0.001–0.8	[26]
Pt_1Pd_1/LMC[c]/GCE	−0.2	0.3	0.0005–27	[27]
PtPd/MWCNTs	0.25	1.2	0.0025–0.125	[28]
Au–Pt NPs/IL[d]/CS/GCE	−0.05	3×10^{-4}	$5–355 \times 10^{-6}$	[29]
PdCo/CNF-CPE	−0.15	0.1	0.0002–23.5	This work

[a] LMC: large mesoporous carbon.
[b] VACNTs: vertically aligned multiwalled carbon nanotubes.
[c] MCNs: mesoporous carbon nanospheres.
[d] IL: ionic liquid.

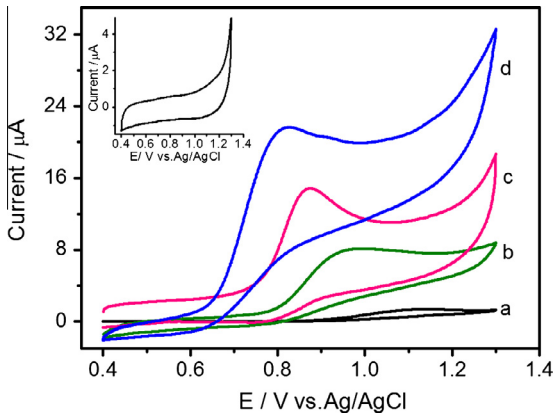

Fig. 5. CVs of CPE (a), Co/CNF-CPE (b), Pd/CNF-CPE (c), and PdCo/CNF-CPE (d) electrodes in 0.1 M PBS (pH 4.0) containing 0.5 mM nitrite. Inset: CV of PdCo/CNF-CPE electrode in black 0.1 M PBS (pH 4.0) solution. Scan rate: 50 mV s^{-1}.

overpotential toward nitrite oxidation at PdCo/CNF-CPE further illustrated that PdCo/CNF were excellent materials for electrochemical sensing.

Fig. S3A displays the typical DPV responses of PdCo/CNF-CPE electrode toward different concentrations of nitrite. A LOD of 0.2 μM ($S/N = 3$) can be achieved, and the calibration curve for nitrite detection was in two ranges of 0.4–30 μM and 30–400 μM with the correlation coefficient of 0.9992 and 0.9990, respectively (Fig. S3B). The LOD is lower than that obtained at the nano-Pt/P3MT modified electrode (1.5 μM) [31], G_4-NH_4/MWNT/GCE electrode (2.0 μM) [32], and thionine modified aligned carbon nanotubes electrode (1.12 μM) [33].

Reproducibility and stability are important parameters to evaluate the applicability of electrochemical sensors. The batch-to-batch reproducibility of the PdCo/CNF-CPE was estimated from the current responses of six different electrodes to 5 μM nitrite. The relative standard deviation (RSD) was calculated to be 4.8%. In addition, the PdCo/CNF-CPE showed a good reproducibility with RSD of 4.5% for 10 successive measurements of 3 μM nitrate. When the electrode was stored in a desicator at room temperature for one month, the current response remained 94% of its initial value, suggesting the good stability of the electrode. In addition, possible interference for the detection of nitrite at PdCo/CNF-CPE was investigated by addition of various species into 0.1 M PBS (pH 4.0) containing 100 μM nitrite. The results showed that most of the ions, such as 100-fold Na^+, K^+, Mg^{2+}, Ca^{2+}, Cu^{2+}, Ag^+, Mn^{2+}, Zn^{2+}, Fe^{3+}, NH^{4+}, NO^{3-}, SO_4^{2-}, and 20-fold CO_3^{2-}, Cl^- and F^- did not interfere with nitrite detection.

In order to verify the reliability of the proposed method, the PdCo/CNF-CPE was applied to analysis of nitrite in pickle samples. The pickle was firstly crushed adequately in the mortar and then mixed with deionized water. Afterward, the mixture was filtered

and separated. The residual solution was added into PBS (pH 4.0) for detection. As can be seen in Table S1, the recovery was 97.8–103.7% with RSD less than 3.25%. Meanwhile, the content of pickle sample obtained from UV–visible experiment was consistent with that of the proposed method, suggesting the strong applicability to real samples.

4. Conclusion

PdCo alloy NP–embedded CNF composite have demonstrated to be a suitable platform for nonenzymatic biosensing. In application to H_2O_2 reduction and nitrite oxidation, the PdCo/CNF-CPE electrode exhibits fast voltammetric response with low overpotential, which is contributed to the synergic effect and firm embedment of well-dispersed PdCo alloy NPs. Particularly, the proposed H_2O_2 and nitrite sensors possesses many attractive analytical performances such as wide linear range, low detection limit, high selectivity with good stability, and strong applicability to real sample, suggesting the potential application of PdCo/CNF for constructing efficient biosensing.

Acknowledgment

We are grateful for the financial support from the National Natural Science Foundation of China (No. 21222505).

Appendix A. Supplementary material

Supplementary data associated with this article can be found, in the online version, at http://dx.doi.org/10.1016/j.jcis.2015.03.014.

References

[1] X. Xu, S.J. Jiang, Z. Hu, S.Q. Liu, ACS Nano 4 (2010) 4292.
[2] S.H. Chen, R. Yuan, Y.Q. Chai, L.Y. Zhang, N. Wang, X.L. Li, Biosens. Bioelectron. 22 (2007) 1268, http://dx.doi.org/10.1016/j.bios.2006.05.022.
[3] B.Q. Wang, B. Li, Z.X. Wang, G.B. Xu, Q. Wang, S.J. Dong, Anal. Chem. 71 (1999) 1935, http://dx.doi.org/10.1021/ac980940q.
[4] W. Chen, S. Cai, Q.Q. Ren, W. Wen, Y.D. Zhao, Analyst 137 (2012) 49, http://dx.doi.org/10.1039/C1AN15738H.
[5] X.Y. Li, X.H. Liu, W.W. Wang, L. Li, X.Q. Lu, Biosens. Bioelectron. 59 (2014) 221, http://dx.doi.org/10.1016/j.bios.2014.03.046.
[6] S.H. Chen, R. Yuan, Y.Q. Chai, F.X. Hu, Microchim. Acta 180 (2013) 15, http://dx.doi.org/10.1007/s00604-012-0904-4.
[7] J.M. You, Y.N. Jeong, M.S. Ahmed, S.K. Kim, H.C. Choi, S. Jeon, Biosens. Bioelectron. 26 (2011) 2287, http://dx.doi.org/10.1016/j.bios.2010.09.053.
[8] M. Han, S. Liu, J.C. Bao, Z.H. Dai, Biosens. Bioelectron. 31 (2012) 151, http://dx.doi.org/10.1016/j.bios.2011.10.008.
[9] F.X. Jiang, R.R. Yue, Y.K. Du, J.K. Xu, P. Yang, Biosens. Bioelectron. 44 (2013) 127, http://dx.doi.org/10.1016/j.bios.2013.01.003.
[10] J. S Huang, D.W. Wang, H.Q. Hou, T.Y. You, Adv. Funct. Mater. 18 (2008) 441, http://dx.doi.org/10.1002/adfm.200700729.
[11] J.A. Rodriguez, D.W. Goodman, Science 257 (1992) 897, http://dx.doi.org/10.1126/science.257.5072.897.
[12] C.Z. Zhu, S.J. Guo, S.J. Dong, Adv. Mater. 24 (2012) 2326, http://dx.doi.org/10.1002/adma.201104951.
[13] X.L. Sun, S.J. Guo, Y. Liu, S.H. Sun, Nano Lett. 12 (2012) 4859, http://dx.doi.org/10.1021/nl302358e.
[14] J.F. Huang, S. Vongehr, S.C. Tang, H.M. Lu, X.K. Meng, J. Phys. Chem. C 14 (2010) 15005, http://dx.doi.org/10.1021/jp104675.
[15] X.F. Yang, J. Hu, J. Fu, R.Q. Wu, B.E. Koel, Angew. Chem. Int. Ed. 50 (2011) 10182, http://dx.doi.org/10.1002/anie.201101251.
[16] D.L. Wang, H.L. Xin, Y.C. Yu, H.S. Wang, E. Rus, D.A. Muller, H.D. Abruña, J. Am. Chem. Soc. 132 (2010) 17664, http://dx.doi.org/10.1021/ja107874u.
[17] V. Mazumder, M.F. Chi, M.N. Mankin, Y. Liu, O. Metin, D.H. Sun, K.L. More, S.H. Sun, Nano Lett. 12 (2012) 1102, http://dx.doi.org/10.1021/nl2045588.
[18] L.Y. Chen, H. Guo, T. Fujita, A. Hirata, W. Zhang, A. Inoue, M.W. Chen, Adv. Funct. Mater. 21 (2011) 4364, http://dx.doi.org/10.1002/adfm.201101227.
[19] D. Liu, Q.H. Guo, H.Q. Hou, O. Niwa, T.Y. You, ACS Catal. 4 (2014) 1825, http://dx.doi.org/10.1021/cs5000153.
[20] Z.X. Wu, Y.Y. Lv, Y.Y. Xia, P.A. Webley, D.Y. Zhao, J. Am. Chem. Soc. 134 (2012) 2236, http://dx.doi.org/10.1021/ja209753.
[21] H.C. Gao, F. Xiao, C.B. Ching, H.W. Duan, ACS Appl. Mater. Inter. 3 (2011) 3049, http://dx.doi.org/10.1021/am200563.
[22] X.M. Zhou, L.Z. Fan, Electrochim. Acta 55 (2010) 8111, http://dx.doi.org/10.1016/j.electacta.2010.02.023.
[23] X.J. Bian, K. Guo, L. Liao, J.J. Xiao, J.L. Kong, C. Ji, B.H. Liu, Talanta 99 (2012) 256, http://dx.doi.org/10.1016/j.talanta.2012.05.048.
[24] B. Xu, M. Ye, Y. Yu, W. Zhang, Anal. Chim. Acta 674 (2010) 20, http://dx.doi.org/10.1016/j.aca.2010.06.004.
[25] Y. Li, J. Zhang, J. Xuan, L. Jiang, J.J. Zhu, Electrochem. Commun. 12 (2010) 777, http://dx.doi.org/10.1016/j.elecom.2010.03.031.
[26] Y. Liu, D.W. Wang, L. Xu, H.Q. Hou, T.Y. You, Biosens. Bioelectron. 26 (2011) 4585, http://dx.doi.org/10.1016/j.bios.2011.05.034.
[27] H. Wang, X.J. Bo, J. Bai, L.X. Wang, L.P. Guo, J. Electroanal. Chem. 662 (2011) 281, http://dx.doi.org/10.1016/j.jelechem.2011.06.020.
[28] K.J. Chen, K. Chandrasekara Pillai, J. Rick, C.J. Pan, S.H. Wang, C.C. Liu, B.J. Hwang, Biosens. Bioelectron. 33 (2012) 120, http://dx.doi.org/10.1016/j.bios.2011.12.037.
[29] F. Xiao, F. Zhao, Y. Zhang, G. Guo, B. Zeng, J. Phys. Chem. C 113 (2009) 849, http://dx.doi.org/10.1021/jp808162.
[30] S.M. Chen, J. Electroanal. Chem. 457 (1998) 23, http://dx.doi.org/10.1016/S0022-0728(98)00143-0.
[31] O.A. Bolade, I.O. Kenneth, N. Tebello, Electrochim. Acta 51 (2006) 6470, http://dx.doi.org/10.1016/j.electacta.2006.04.033.
[32] N.N. Zhu, Q. Xu, S.N. Li, H. Gao, Electrochem. Commun. 11 (2009) 2308, http://dx.doi.org/10.1016/j.elecom.2009.10.018.
[33] K. Zhao, H.Y. Song, S.Q. Zhuang, L.M. Dai, P.G. He, Y.Z. Fang, Electrochem. Commun. 9 (2007) 65, http://dx.doi.org/10.1016/j.elecom.2006.07.001.